



OPEN

Ag nanoparticles immobilized on new magnetic algininate halloysite as a recoverable catalyst for reduction of nitroaromatics in aqueous media

Pourya Mohammadi, Majid Heravi✉ & Mansoureh Daraie

Amines can be applied in the synthesis of various important compounds such as dyes, drugs, polymers, pharmaceutical products, and biologically active materials. The significant subject in the preparation of amines is the selection of the most effective heterogeneous catalyst to get the best catalytic efficiency, stability, recoverability, and reusability. For this target, we prepared new algininate magnetically recoverable nanocatalyst by stabilization of Ag nanoparticles on the surface of the halloysite (HS) [HS-Alginate-Ag/Fe₃O₄]. Several detection methods confirmed the production of HS-Alginate-Ag/Fe₃O₄ nanocatalyst and the results obtained were well explained in the context. HS-Alginate-Ag/Fe₃O₄ presented good catalytic performance for the hydrogenation of nitro compounds using NaBH₄ as the reducing agent and hydrogen donor. The good activity and durability of this catalyst can be attributed to the good dispersion and nano-sized particle of silver nanoparticles.

The selective hydrogenation of nitro compounds to the corresponding amino compounds is one of the main synthetic processes from the industrial and academic fields because the obtained amines are commercially valuable starting materials and adaptable intermediates in the production of pharmaceuticals, rubber auxiliaries, dyestuffs, explosives, antioxidants, pesticides, agrochemicals, spices, polymers, and drugs^{1–4} while nitro compounds are the carcinogenic contaminants and toxic bio-refractories entered in industrial and agricultural wastewater⁵. Therefore, finding effective methods to eliminate these pollutants is essential. In this regard, various reduction systems and catalysts have been applied for the reduction of nitro compounds^{6–8}. The classic method of synthesizing amine compounds is to reduce nitro compounds by metallic reagents, which resulting in considerable pollution in the environment⁹. However, this method has various disadvantages, such as simple corrosion of equipment, environmentally hazardous, low performance, and difficulties in continuous products and their separation¹⁰. Hence, synthetic processes including cheaper and clearer alternatives are required. There are several methods for the reduction of nitro compounds including chemical reduction, electro-reduction, and chemical hydrogenation¹¹. Among them, the catalytic hydrogenation of these compounds has received special attention owing to its excellent performance and selectivity. One of these methods is the use of NaBH₄ in water as a hydride source. However, reducing nitro groups with NaBH₄ in the lack of catalysts is very time-consuming and tedious, so various metal catalysts have been utilized to perform this reduction^{12–14}.

Recently, metal-based nanoparticles synthesized via the green process without any stabilization agent are broadly employed in heterogeneous and homogeneous catalysis systems because of their particular structures and characteristics^{4,15}. The use of metal nanoparticles as the nanocatalyst in the presence of NaBH₄ as a hydride donor is an eco-friendly approach for the hydrogenation of nitro compounds because this reaction can be done under moderate conditions without acid sewage¹⁶. Among metallic nanoparticles, silver nanoparticles have interested very consideration due to their good catalytic activities, extremely large surface area, excellent conductivity, and high stability^{17,18}. Such catalytic systems provide highly effective and selective organic reactions. Although Ag nanoparticles as catalysts have various benefits, great cost, aggregation, and problems in recovery are the apparent difficulties to be faced. Nowadays, an improved approach is to deposit these nanoparticles on

Department of Chemistry, Faculty of Physics and Chemistry, Alzahra University, Vanak, PO Box 1993891176, Tehran, Iran. ✉email: mmh1331@yahoo.com

appropriate supports¹⁹. Since some supports are costly for practical application, hence, finding affordable and accessible support is necessary.

Halloysite (HS) has the potential to be used as a catalyst carrier to inhibit the aggregation of silver nanoparticles. HS with a formula $\text{Al}_2\text{Si}_2\text{O}_5(\text{OH})_4 \cdot n\text{H}_2\text{O}$ ($n = 0, 2$) is naturally existing in soils and weathered rocks^{20,21}. It is a clay mineral having a hollow tubular structure with a multi-layer wall in the nanometer range (lengths of 300 ~ 900 nm, inside diameters of 10 ~ 25 nm, and outside diameters of 50 ~ 100 nm) and a high specific surface area^{22,23}. As well as HS owns many reactive groups on inside and outside surfaces^{24–26}. In comparison with other tubular nanostructures e.g. carbon nanotubes, HS is eco-friendly, biocompatible, and cost-effective. Due to its high specific surface area and hollow structure, HS can serve as promising support for various applications^{27–30}. HS has been investigated as high-efficiency support for various nanoparticle such as Pd³¹, ZnO³², TiO₂³³, Au³⁴ resulting in effective catalyzes with adjustable properties.

In recent years, polysaccharides including chitosan, gelatin, and alginate are investigated as a most appropriate substrate for metal nanoparticles owing to their biocompatible, biodegradable, rheological, and non-toxic features^{35–38}. Among them, alginate is a non-toxic and anionic compound, naturally existing in bacteria and brown algae. Its polysaccharide chain contains β -D-mannuronate (M) and α -L-guluronate (G), linearly linked by 1,4-glycosidic units³⁹. Moreover, there are abundant of hydroxyl and carboxyl groups in this macromolecule which can be suitably connected to other compounds.

Over the last years, magnetic nanoparticles (e.g. Fe₃O₄) have been broadly studied as a suitable compound for the separation of compounds in numerous biological and industrial fields⁴⁰. Their magnetic property are them effectively and readily separated from the reaction media by using an external magnet.

In this study, we describe the synthesis of Ag nanoparticles stabilized on new alginate magnetic halloysite as a magnetically separable nanocatalyst and it was also investigated for its catalytic activity in hydrogenation of nitro aromatic compounds with NaBH₄ as a mild hydride donor. It is found that the as-synthesized HS-Alginate-Ag/Fe₃O₄ can be used as a new, reusable and efficient nanocatalyst for the reduction of nitro aromatic compounds into the target amine derivatives. To the best of our knowledge, HS-Alginate-Ag/Fe₃O₄ has not been reported as the nanocatalyst for the reduction of nitro aromatic compounds so far.

Experimental

Materials and instruments. All the chemical material and solvents such as acetonitrile (CH₃CN, 99%), ethanol (CH₃CH₂OH, 96%), dichloromethane (CH₂Cl₂, 99%), N, N-Dimethylformamid (HCON (CH₃)₂, DMF, 99.8%), and ammonia solution (NH₄OH, 25%) were used with high purity from Merck. The required chemicals such as iron (III) chloride and iron (II) (FeCl₃·6H₂O, 97% and FeCl₂·4H₂O, 99%), Sodium borohydride (NaBH₄, 98%), silver nitrate (AgNO₃, 99%), halloysite, alginate, and nitroaromatic derivations were prepared from Sigma-Aldrich.

For determining the crystalline and phase structure of the synthesized nanocomposite, Transmission electron microscopy (TEM) imaging was performed with a CM30, Philips, Germany operating at 300 kV. Field emission scanning electron microscopy (FESEM) images equipped with an EDS attachment were taken on VEGA3, Tecscan, USA. X-ray diffraction patterns were obtained on a PW 1800 X-ray diffractometer (Philips, Netherlands) with Cu K α radiation ($\lambda = 0.154056$ nm). Fourier transform infrared (FTIR) spectra were recorded using an FTIR apparatus (SHIMADZU, Japan) and in the range of 4000–400 cm⁻¹.

Synthesis of HS-Alginate-Ag/Fe₃O₄ nanocatalyst. The synthesis of HS-Alginate-Ag/Fe₃O₄ nanocomposites involves several steps as follows (Fig. 1):

- Synthesis of Hs-Fe₃O₄: The 2.5 g of the HS was dispersed in 120 mL of deionized water for 15 min. Then, iron (III) chloride (1.37 g) and iron (II) (0.5 g) were added to the above suspension. This suspension was stirred at 70 °C under an N₂ atmosphere. Then, 11 mL of concentrated ammonia was added to the above mixture and stirred for one hour. At the completion of the reaction, the product by an external magnet was separated, washed 3 times with distilled water, and dried at room temperature.
- Synthesis of HS-Alginate/Fe₃O₄: In this stage, 500 mg of halloysite/Fe₃O₄ in 60 mL was dispersed in water for 20 min. Then 100 mg of alginate was added to the above solution and stirred for 5 h. Finally, the precipitation by using an external magnet was separated, washed 3 times with distilled water, and dried at room temperature.
- Synthesis of HS-Alginate-Ag/Fe₃O₄: At first, 500 mg of HS-Alginate/Fe₃O₄ in 50 mL of water was stirred for 90 min at 25 °C, and then 1.4 mmol AgNO₃ was added to the above mixture. In the next step, 0.25 mL of hydrazine hydrate in 1 mL of distilled water was added dropwise to the above solution and stirred at 25 °C for overnight. Subsequently, the precipitation by a magnet was isolated and washed three times with distilled water, and dried completely.

The procedure for reduction of nitro aromatic compounds. To a round bottomed flask containing nitro compound (1 mmol) and 5 mL H₂O, 0.03 g catalyst was added and the mixture was vigorously stirred at room temperature. Then NaBH₄ was added to the suspension and the reaction temperature was raised to 50 °C. After completion of the reaction (monitored by TLC), the catalyst by an external magnetic was separated and then the precipitate was recrystallized from EtOH to give pure products (Table 2).

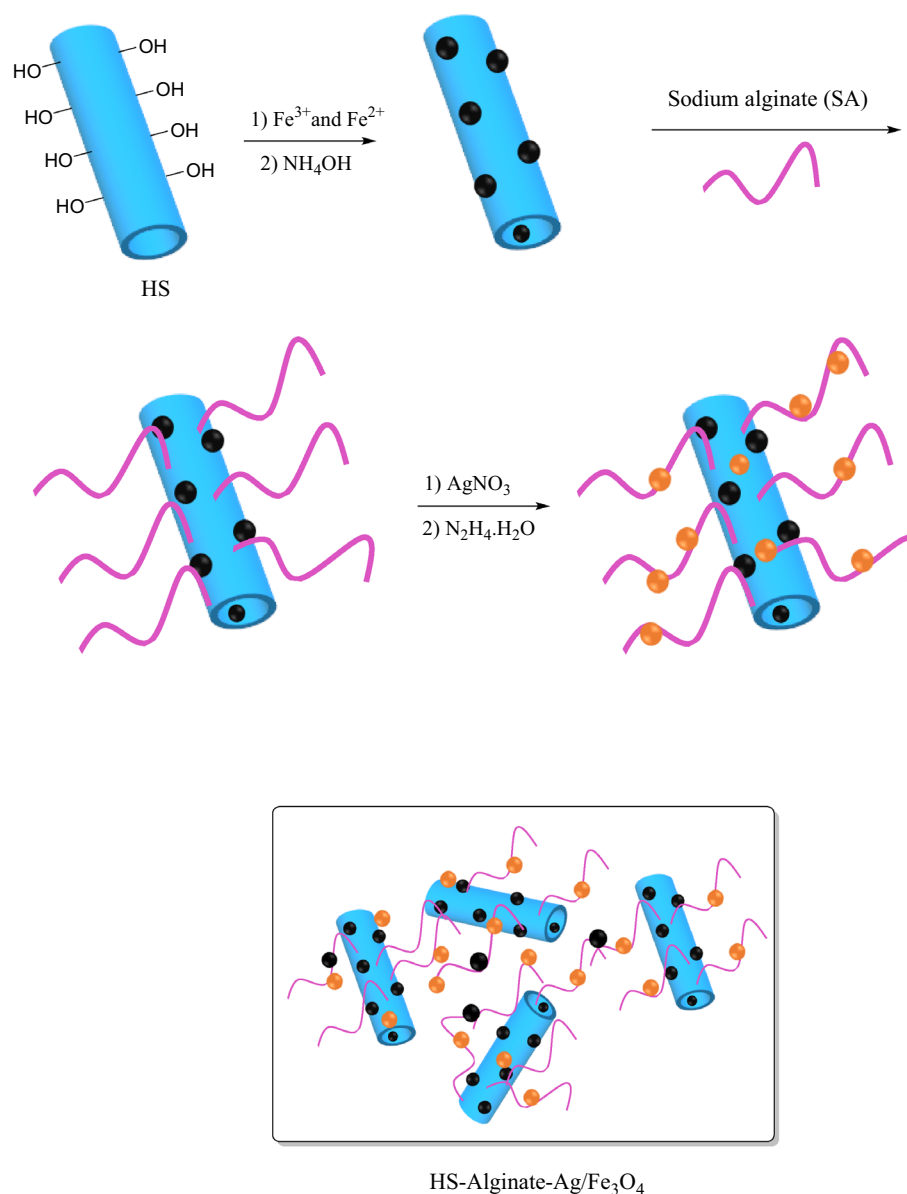


Figure 1. The nanocatalyst synthesis pathway (drawn with ChemDraw Pro 12.0 software (<https://en.freedownloadmanager.org/Windows-PC/ChemDraw-Pro.html>)).

Result and discussion

Catalyst formation verification. XRD analyses authenticate the Fe_3O_4 nanoparticles and HS-Alginate-Ag/ Fe_3O_4 nanocomposite as presented in Fig. 2. As shown in Fig. 2a, the diffraction peaks at $2\theta = 30.79^\circ$, 36.14° , 44.09° , 57.89° , and 63.04° corresponding to the Fe_3O_4 nanoparticles interlayer spacing (220), (311), (400), (511), and (440) reflection plane, respectively. In Fig. 2b, in addition to peaks related to Fe_3O_4 nanoparticles, the diffraction peaks at $2\theta = 12.74^\circ$, 20.84° , 25.24° , and 55.84° correspond to the HS interlayer spacing (001), (110), (002), and (114) reflection plane, respectively. In addition, the diffraction peaks at 38.54° , 44.09° , 63.04° , and 78.09° , correspond to the Ag nanoparticles interlayer spacing (111), (200), (220), and (311) reflection plane, respectively.

FTIR spectra of HS/ Fe_3O_4 , HS-Alginate/ Fe_3O_4 , and HS-Alginate-Ag/ Fe_3O_4 were recorded, Fig. 3. In the FTIR spectrum of HS/ Fe_3O_4 (Fig. 3a), the typical adsorption peaks of Si–O stretching located at 1091 cm^{-1} . The vibrations at 534 cm^{-1} are assigned to the Al–O–Si group. In addition, the absorption bands at 3695 cm^{-1} and 3624 cm^{-1} are ascribed to vibrations of the inner-surface hydroxyl groups. And two apparent peaks at 585 , and 635 cm^{-1} were assigned to the stretching vibration of the Fe–O groups in the Fe_3O_4 units. In addition to the characteristic peaks of HS and Fe_3O_4 , the FTIR spectra of HS-Alginate/ Fe_3O_4 (Fig. 3b) present the notable peak at 1640 cm^{-1} is owing to the C=O stretching of the alginic acid unit, as well as the peak at 2978 cm^{-1} , can be attributed to the C–H stretching vibrations from the alginate backbone. In the FTIR spectrum of HS-Alginate-Ag/

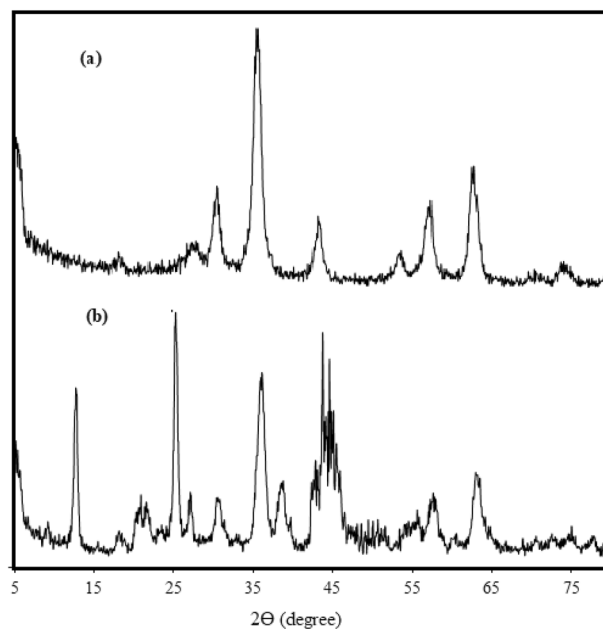


Figure 2. XRD patterns of (a) Fe₃O₄, and (b) HS-Alginate-Ag/Fe₃O₄ nanocomposite.

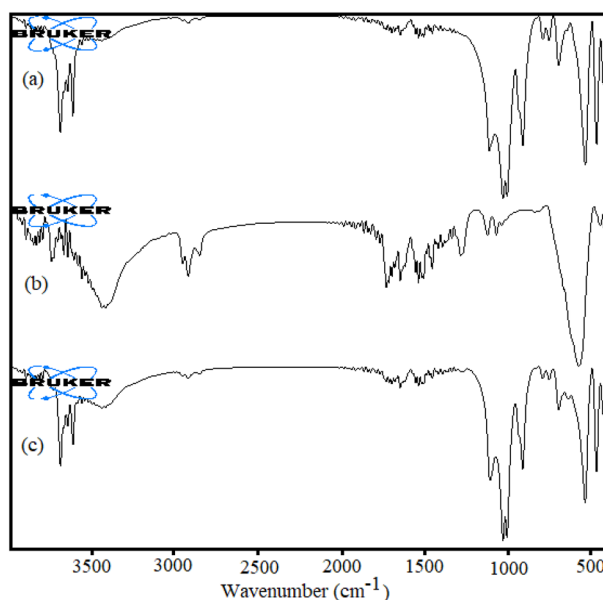


Figure 3. FTIR spectra of (a) HS-Fe₃O₄, (b) HS-Alginate/Fe₃O₄, and (c) HS-Alginate-Ag/Fe₃O₄.

Fe₃O₄ nanocomposite, all of the typical peaks of HS, alginate, and Fe₃O₄ can be definitely distinguished, such as the C–O and –OH vibrations, and Si–O, Al–O–H stretching vibrations (Fig. 3c). However, several shifts are also observed. These shifts can be recognized as an indication that the hydroxyl and carboxyl groups are responsible for the Ag nanoparticle stabilization.

The morphology and chemical composition of HS-Alginate-Ag/Fe₃O₄ were determined through FESEM, EDS, mapping, and TEM. As shown in Figs. 4 and 5 it was clear that HS has a diameter in the range of 41–52 nm, and the HS nanotubes were open-ended. In the FESEM image, it can be revealed some roughness on the surface of HS owing to grafted alginate. Also, the HS structures have a slight agglomeration. However, it showed that its surface morphology does not change very in the presence of Fe₃O₄ and Ag (Fig. 4a). As can be observed in Fig. 5, the HS-Alginate-Ag/Fe₃O₄ nanocatalyst has an almost uniform size distribution. The EDS (Fig. 4b) represented that the constituents for the HS-Alginate-Ag/Fe₃O₄ were Al, Si, O, Ag, C, and Fe. According to mapping (Fig. 4c), these elements were irregularly dispersed on the surface of HNTs.

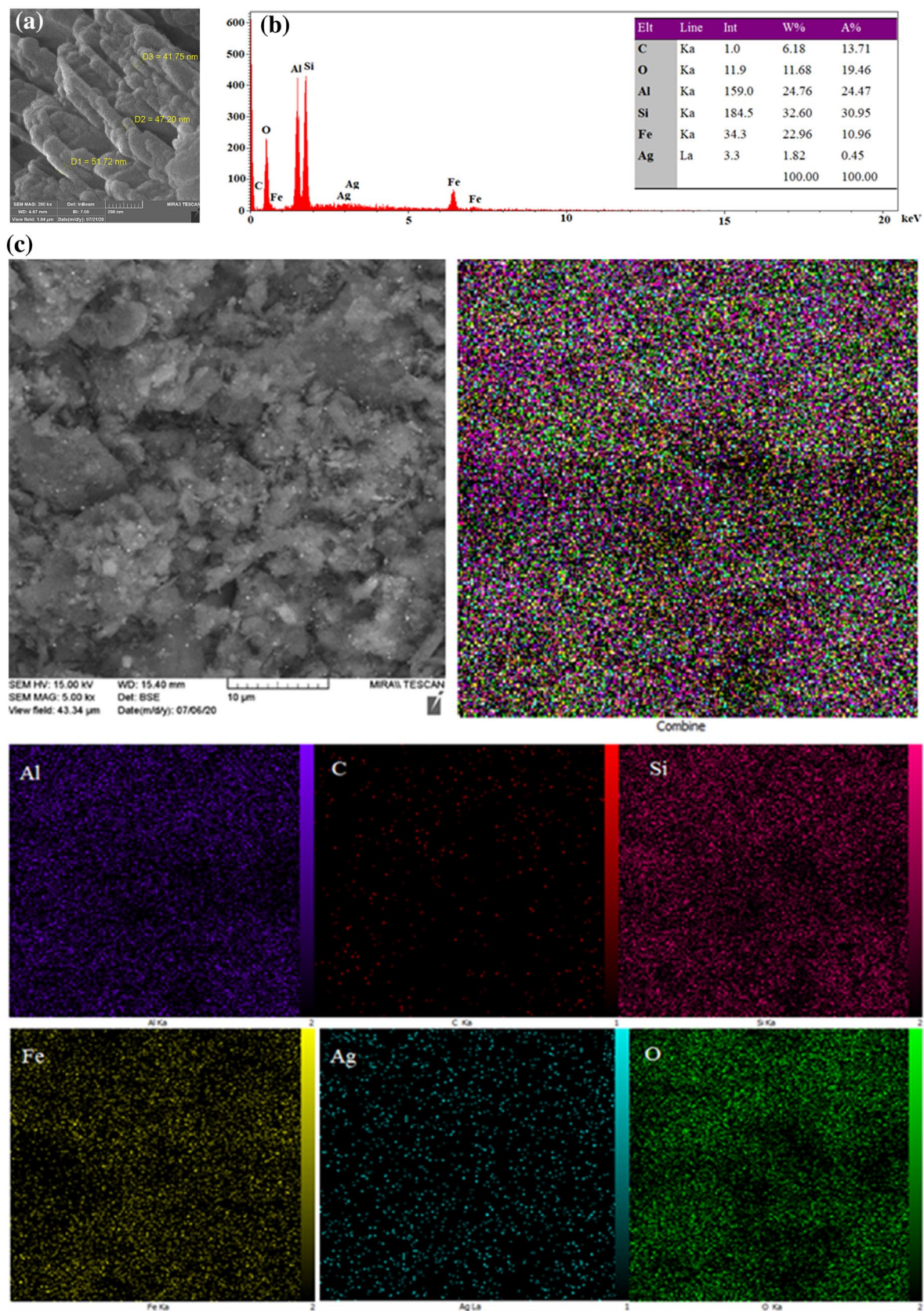


Figure 4. (a) FESEM images, (b) EDS, (c) Mapping of HS-Alginate-Ag/Fe₃O₄.

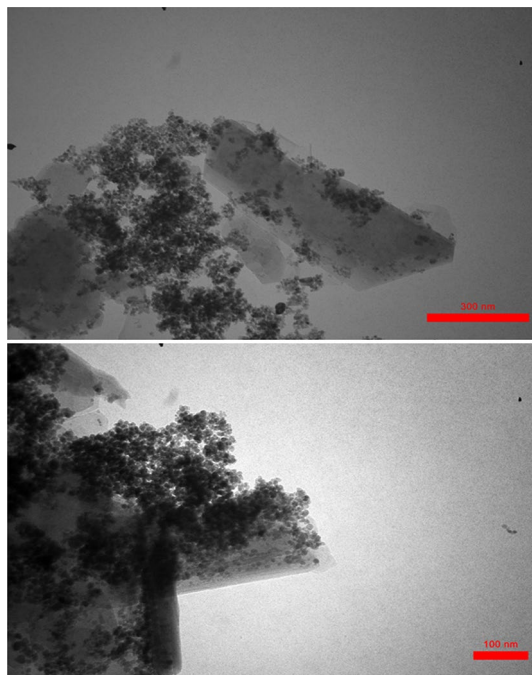


Figure 5. TEM images of HS-Alginate-Ag/Fe₃O₄.

Entry	Catalyst amount (g)	solvent	Temperature (°C)	Time (min)	Yield (%)
1	0.04	CH ₃ CN	50	40	10
2	0.04	CH ₂ Cl ₂	Reflux	45	Trace
3	0.04	DMF	50	40	10
4	0.04	EtOH	50	30	70
5	0.04	H ₂ O	Reflux	30	85
6	0.04	H ₂ O	70	35	70
7	0.04	H₂O	50	30	100
8	0.04	H ₂ O	r.t	45	45
9	0.03	H ₂ O	50	30	95
10	0.05	H ₂ O	50	30	100

Table 1. Optimization conditions for reduction of nitro aromatic compounds. Bold indicates the optimal values of the reaction conditions

The TEM image in Fig. 5 shows a defect in the HS surface that results in rough exterior walls, which is consistent with the FESEM image. The strong interaction of the polymer between the substrate (halloysite) and the nanoparticles, especially the Fe₃O₄ nanoparticles due to the carboxylic acid functional groups, as well as the flexibility of the polymer, has caused the nanoparticle and polymer images to be seen as mixtures that are almost far apart. This could be because polymers are also present between halloysites.

Investigation of the catalytic activity of HS-Alginate-Ag/Fe₃O₄. Subsequently, hydrogenation of nitrobenzene was selected as the model reaction to investigate the catalytic activity of the HS-Alginate-Ag/Fe₃O₄. Therefore, the model reaction was firstly tested in the presence of (0.04 g) at 70 °C in H₂O as solvent that was mild and environmentally benign conditions. Such conditions gave aniline in 50% yields after 1 h. To improve the yield of model reaction and decrease its time, the used solvent, the amount of HS-Alginate-Ag/Fe₃O₄, and the temperature were changed. It was found that running the reaction at ambient temperature gives the desired products in higher yields. By studying more temperatures, 50 °C was chosen as the optimized reaction temperature. Accordingly, by investigating the amounts of HS-Alginate-Ag/Fe₃O₄, it was found that the optimized amount is 0.04 g HS-Alginate-Ag/Fe₃O₄ and further escalation didn't increase the product yield. Furthermore, among the tested solvents, water was the best one. Under the optimized conditions, hydrogenation of nitrobenzene gave anilines in 100% yields, respectively, after 30 min (Table 1, entry 7).

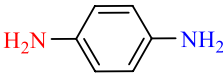
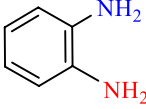
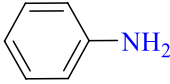
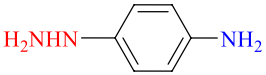
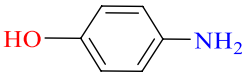
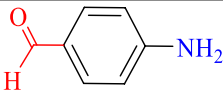
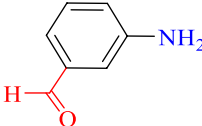
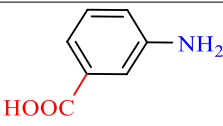
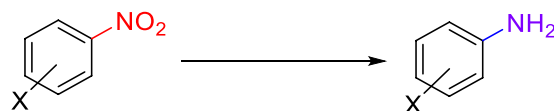
Entry	Product	Time (min)	Yield (%)	Melting point (Abs./ Lit.) ¹
1		25	100	143–144/145–147
2		32	99	100–103/102–104
3		30	100	187/184 (boiling point)
4		60	92	18–19/19–20
5		60	90	187/186–190
6		30	100	78/77–79
7		35	100	29–30/28–30
8		120	95	180/187–189
9	C ₂ H ₅ -NH ₂	40	96	20–21/19–20

Table 2. Reduction of aromatic nitro compounds in the presence of HS-Alginate-Ag/Fe₃O₄ and NaBH₄.



The generality of this protocol was then examined using different starting materials to produce various aromatic amines. The results confirmed that HS-Alginate-Ag/Fe₃O₄ can catalyze the hydrogenation reaction of all applied substrates to give the corresponding amine compounds at short reaction times and in high efficiencies (Table 2).

Kinetic study. The catalytic reduction of 4-nitrophenol was selected as a model reaction to appraise the catalytic activity of the HS-Alginate-Ag/Fe₃O₄ nanocatalysts. UV–Vis absorption spectra were used to monitor the concentration changes. The kinetics of this reaction was investigated with HS-Alginate-Ag/Fe₃O₄ nanocatalyst. It followed the pseudo-first-order kinetics concerning the concentration of 4-nitrophenol as follows:

$$\ln \frac{C_t}{C_0} = -kt$$

where C_t and C_0 are the 4-nitrophenol concentrations at time t and at the beginning time, respectively, and k is the apparent rate constant. The plot of $\ln(C_t/C_0)$ vs time was obtained and a good linear correlation was observed (0.99). This phenomenon also showed that this reaction followed pseudo-first-order kinetics. From the slope of this equation, the apparent rate constant (K) for the reduction of 4-nitrophenol was obtained of 0.047 s^{-1} ^{41,42}.

Study of reusability. The results obtained from the reusability evaluation of HS-Alginate-Ag/Fe₃O₄ in the model reaction are as follows. By completion of each cycle, the catalyst was separated, rinsed with EtOH, dried and reused in the next cycle. As shown by the results in Fig. 6, recycling the catalyst up to 6 runs showed no important loss of its catalytic activity. Since the catalyst contains magnetic Fe₃O₄ nanoparticles, it is easily sepa-

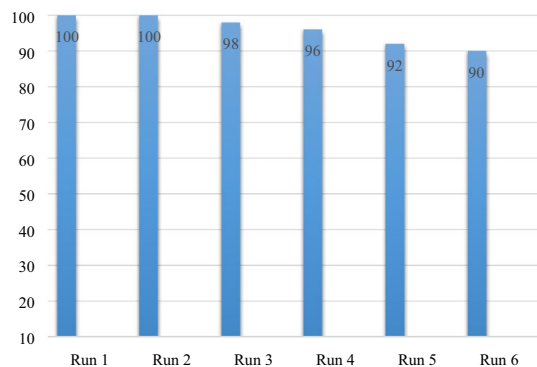


Figure 6. Reusability test of the HS-Alginate-Ag/Fe₃O₄ for model reaction.

rated from the reaction mixture by an external magnetic field. Now, after six times of recovery, observing good efficiency as well as ICP (Ag content: 1.2% to 1.1% after 6 times) results showed that the catalyst has good magnetic properties and high stability.

Conclusions

The construction of cost-effective and reusable catalytic systems by using low-priced compounds and simple methods is an attractive research field for organic chemists. This study focused on the modification of halloysite material through three strategies including doping of alginate, deposition of silver nanoparticles, and Fe₃O₄ dispersion on the support surface which was synthesized for the first time. The as-prepared HS-Alginate-Ag/Fe₃O₄ was utilized as a suitable and recoverable nanocatalyst for the reduction of nitro aromatic compounds to the related amine compounds. The obtained HS-Alginate-Ag/Fe₃O₄ nanocatalyst presented a good performance in the reduction of nitro aromatic compounds to the amine aromatic compounds for a broad range of materials under moderate conditions. Recycling experiment of HS-Alginate-Ag/Fe₃O₄ was performed using water as a green solvent and NaBH₄ as a hydrogen donor. This heterogeneous HS-Alginate-Ag/Fe₃O₄ nanocatalyst exhibited acceptable stability and recovered by a magnet and reutilized several times with a low decrease in its efficiency.

Received: 9 January 2021; Accepted: 10 August 2021

Published online: 24 August 2021

References

- Gholinejad, M., Zareh, F. & Nájera, C. Nitro group reduction and Suzuki reaction catalysed by palladium supported on magnetic nanoparticles modified with carbon quantum dots generated from glycerol and urea. *Appl. Organomet. Chem.* **32**(1), e3984 (2018).
- Ma, X., Zhou, Y. X., Liu, H., Li, Y. & Jiang, H. L. A MOF-derived Co-CoO@N-doped porous carbon for efficient tandem catalysis: Dehydrogenation of ammonia borane and hydrogenation of nitro compounds. *Chem. Commun.* **52**(49), 7719–7722 (2016).
- Rahman, A. & Jonnalagadda, S. B. Swift and selective reduction of nitroaromatics to aromatic amines with Ni-boride-silica catalysts system at low temperature. *Catal. Lett.* **123**(3–4), 264–268 (2008).
- Sadjadi, S., Lazzara, G., Heravi, M. M. & Cavallaro, G. Pd supported on magnetic carbon coated halloysite as hydrogenation catalyst: Study of the contribution of carbon layer and magnetization to the catalytic activity. *Appl. Clay Sci.* **182**, 105299 (2019).
- Hernández-Gordillo, A. & González, V. R. Silver nanoparticles loaded on Cu-doped TiO₂ for the effective reduction of nitroaromatic contaminants. *Chem. Eng. J.* **261**, 53–59 (2015).
- Wu, F., Qiu, L. G., Ke, F. & Jiang, X. Copper nanoparticles embedded in metal-organic framework MIL-101 (Cr) as a high performance catalyst for reduction of aromatic nitro compounds. *Inorg. Chem. Commun.* **32**, 5–8 (2013).
- Nandanwar, S. U. & Chakraborty, M. Synthesis of colloidal CuO/γ-Al₂O₃ by microemulsion and its catalytic reduction of aromatic nitro compounds. *Chin. J. Catal.* **33**(9–10), 1532–1541 (2012).
- Kalbasi, R. J., Nourbakhsh, A. A. & Babaknezhad, F. Synthesis and characterization of Ni nanoparticles-polyvinylamine/SBA-15 catalyst for simple reduction of aromatic nitro compounds. *Catal. Commun.* **12**(11), 955–960 (2011).
- Cui, X. *et al.* Cobalt nanoparticles supported on N-doped mesoporous carbon as a highly efficient catalyst for the synthesis of aromatic amines. *J. Colloid Interface Sci.* **501**, 231–240 (2017).
- Shukla, A., Singha, R. K., Sasaki, T. & Bal, R. Nanocrystalline Pt-CeO₂ as an efficient catalyst for a room temperature selective reduction of nitroarenes. *Green Chem.* **17**(2), 785–790 (2015).
- Aditya, T., Pal, A. & Pal, T. Nitroarene reduction: A trusted model reaction to test nanoparticle catalysts. *Chem. Commun.* **51**(46), 9410–9431 (2015).
- Mei, Y. *et al.* High catalytic activity of platinum nanoparticles immobilized on spherical polyelectrolyte brushes. *Langmuir* **21**(26), 12229–12234 (2005).
- Dotzauer, D. M., Bhattacharjee, S., Wen, Y. & Bruening, M. L. Nanoparticle-containing membranes for the catalytic reduction of nitroaromatic compounds. *Langmuir* **25**(3), 1865–1871 (2009).
- Kuroda, K., Ishida, T. & Haruta, M. Reduction of 4-nitrophenol to 4-aminophenol over Au nanoparticles deposited on PMMA. *J. Mol. Catal. A* **298**(1–2), 7–11 (2009).
- Sravanthi, K., Ayodhya, D. & Swamy, P. Y. Green synthesis, characterization and catalytic activity of 4-nitrophenol reduction and formation of benzimidazoles using bentonite supported zero valent iron nanoparticles. *Mater. Sci. Energy Technol.* **2**(2), 298–307 (2019).
- Qiu, X., Liu, Q., Song, M. & Huang, C. Hydrogenation of nitroarenes into aromatic amines over Ag@BCN colloidal catalysts. *J. Colloid Interface Sci.* **477**, 131–137 (2016).

17. Rostami-Vartooni, A., Nasrollahzadeh, M. & Alizadeh, M. Green synthesis of seashell supported silver nanoparticles using Bunium persicum seeds extract: Application of the particles for catalytic reduction of organic dyes. *J. Colloid Interface Sci.* **470**, 268–275 (2016).
18. Shiraishi, Y. & Toshima, N. Oxidation of ethylene catalyzed by colloidal dispersions of poly (sodium acrylate)-protected silver nanoclusters. *Colloids Surf. A* **169**(1–3), 59–66 (2000).
19. Yan, H. *et al.* General synthesis of high-performing magneto-conjugated polymer core-shell nanoparticles for multifunctional theranostics. *Nano Res.* **10**(2), 704–717 (2017).
20. Zhang, J. *et al.* Preparation and characterization of novel polyethersulfone hybrid ultrafiltration membranes bending with modified halloysite nanotubes loaded with silver nanoparticles. *Ind. Eng. Chem. Res.* **51**(7), 3081–3090 (2012).
21. Lisuzzo, L., Cavallaro, G., Milioto, S. & Lazzara, G. Layered composite based on halloysite and natural polymers: A carrier for the pH controlled release of drugs. *New J. Chem.* **43**(27), 10887–10893 (2019).
22. Pan, J. *et al.* Selective recognition of 2, 4, 6-trichlorophenol by molecularly imprinted polymers based on magnetic halloysite nanotubes composites. *J. Phys. Chem. C* **115**(13), 5440–5449 (2011).
23. Bates, T. F., Hildebrand, F. A. & Swineford, A. Morphology and structure of endellite and halloysite. *Am. Miner.* **35**(7–8), 463–484 (1950).
24. Lvov, Y., Wang, W., Zhang, L. & Fakhrullin, R. Halloysite clay nanotubes for loading and sustained release of functional compounds. *Adv. Mater.* **28**(6), 1227–1250 (2016).
25. Lvov, Y. & Abdullayev, E. Functional polymer-clay nanotube composites with sustained release of chemical agents. *Prog. Polym. Sci.* **38**(10–11), 1690–1719 (2013).
26. Liu, M., Jia, Z., Jia, D. & Zhou, C. Recent advance in research on halloysite nanotubes-polymer nanocomposite. *Prog. Polym. Sci.* **39**(8), 1498–1525 (2014).
27. Zeng, G. *et al.* Novel halloysite nanotubes intercalated graphene oxide based composite membranes for multifunctional applications: Oil/water separation and dyes removal. *Ind. Eng. Chem. Res.* **56**(37), 10472–10481 (2017).
28. Hebbar, R. S., Isloor, A. M., Ananda, K. & Ismail, A. F. Fabrication of polydopamine functionalized halloysite nanotube/polyetherimide membranes for heavy metal removal. *J. Mater. Chem. A* **4**(3), 764–774 (2016).
29. Ghanbari, M. *et al.* Synthesis and characterization of novel thin film nanocomposite (TFN) membranes embedded with halloysite nanotubes (HNTs) for water desalination. *Desalination* **358**, 33–41 (2015).
30. Hashemifard, S. A., Ismail, A. F. & Matsuura, T. Mixed matrix membrane incorporated with large pore size halloysite nanotubes (HNT) as filler for gas separation: Experimental. *J. Colloid Interface Sci.* **359**(2), 359–370 (2011).
31. Zhang, Y., He, X., Ouyang, J. & Yang, H. Palladium nanoparticles deposited on silanized halloysite nanotubes: Synthesis, characterization and enhanced catalytic property. *Sci. Rep.* **3**(1), 1–6 (2013).
32. Li, J. *et al.* Enhanced photocatalytic activity of gC₃N₄-ZnO/HNT composite heterostructure photocatalysts for degradation of tetracycline under visible light irradiation. *RSC Adv.* **5**(111), 91177–91189 (2015).
33. Li, C., Wang, J., Feng, S., Yang, Z. & Ding, S. Low-temperature synthesis of heterogeneous crystalline TiO₂-halloysite nanotubes and their visible light photocatalytic activity. *J. Mater. Chem. A* **1**(27), 8045–8054 (2013).
34. Gómez, L., Hueso, J. L., Ortega-Liébana, M. C., Santamaría, J. & Cronin, S. B. Evaluation of gold-decorated halloysite nanotubes as plasmonic photocatalysts. *Catal. Commun.* **56**, 115–118 (2014).
35. Schexnailder, P. & Schmidt, G. Nanocomposite polymer hydrogels. *Colloid Polym. Sci.* **287**(1), 1–1 (2009).
36. Vieira, E. F., Cestari, A. R., Airolidi, C. & Loh, W. Polysaccharide-based hydrogels: Preparation, characterization, and drug interaction behaviour. *Biomacromol* **9**(4), 1195–1199 (2008).
37. Boanini, E., Rubini, K., Panzavolta, S. & Bigi, A. Chemico-physical characterization of gelatin films modified with oxidized alginate. *Acta Biomater.* **6**, 383–388 (2010).
38. Zhao, P. *et al.* Characterisation and saccharide mapping of polysaccharides from four common Polygonatum spp. *Carbohydr. Polym.* **233**, 115836 (2020).
39. Paques, J. P., van der Linden, E., van Rijn, C. J. & Sagis, L. M. Preparation methods of alginate nanoparticles. *Adv. Colloid Interface Sci.* **209**, 163–171 (2014).
40. Kumar, K. S., Kumar, V. B. & Paik, P. Recent advancement in functional core-shell nanoparticles of polymers: Synthesis, physical properties, and applications in medical biotechnology. *J. Nanopart.* <https://doi.org/10.1155/2013/672059> (2013).
41. Guan, H. *et al.* PtNi nanoparticles embedded in porous silica microspheres as highly active catalysts for p-nitrophenol hydrogenation to p-aminophenol. *J. Chem. Sci.* **128**(9), 1355–1365 (2016).
42. Shang, H., Du, L., Guan, H., Zhang, B. & Xiang, X. Ternary composite of biomass porous Carbon/SnO₂/Pt: An efficient catalyst for reduction of aromatic nitro compounds. *ChemistrySelect* **3**(18), 5066–5072 (2018).

Acknowledgements

The authors appreciate Alzahra University for full support.

Author contributions

P.M.: Visualization, Writing original draft, Formal analysis. M.H.: Fundingacquisition, Methodology, Supervision. M.D.: Methodology.

Competing interests

The authors declare no competing interests.

Additional information

Correspondence and requests for materials should be addressed to M.H.

Reprints and permissions information is available at www.nature.com/reprints.

Publisher's note Springer Nature remains neutral with regard to jurisdictional claims in published maps and institutional affiliations.



Open Access This article is licensed under a Creative Commons Attribution 4.0 International License, which permits use, sharing, adaptation, distribution and reproduction in any medium or format, as long as you give appropriate credit to the original author(s) and the source, provide a link to the Creative Commons licence, and indicate if changes were made. The images or other third party material in this article are included in the article's Creative Commons licence, unless indicated otherwise in a credit line to the material. If material is not included in the article's Creative Commons licence and your intended use is not permitted by statutory regulation or exceeds the permitted use, you will need to obtain permission directly from the copyright holder. To view a copy of this licence, visit <http://creativecommons.org/licenses/by/4.0/>.

© The Author(s) 2021